J Math Chem (2013) 51:2514–2541
DOI 10.1007/s10910-013-0226-8

ORIGINAL PAPER

Noise-assisted quantum electron transfer in photosynthetic complexes

Alexander I. Nesterov · Gennady P. Berman · José Manuel Sánchez Martínez · Richard T. Sayre

Received: 31 May 2013 / Accepted: 2 July 2013 / Published online: 18 July 2013

Abstract Electron transfer (ET) between primary electron donor and acceptor is modeled in the photosynthetic complexes. Our model includes (i) two discrete energy levels associated with donor and acceptor, which are directly interacting and (ii) two continuum manifolds of electron energy levels ("sinks"), each interacting with the donor and acceptor. We also introduce external (classical) noise which acts on both donor and acceptor. We derive a closed system of integro-differential equations which describes the non-Markovian quantum dynamics of the ET. A region of parameters is found in which the ET dynamics can be simplified, and described by coupled ordinary differential equations. Using these simplified equations, both cases of sharp and flat redox potentials are analyzed. We analytically and numerically obtain the characteristic parameters that optimize the ET rates and efficiency in this system. In particular, we demonstrate that even for flat redox potential a simultaneous influence of sink and noise can significantly increase the efficiency of the ET. We discuss a relation between our approach and the Marcus theory of ET.

A. I. Nesterov (✉) · J. M. Sánchez Martínez
Departamento de Física, CUCEI, Universidad de Guadalajara, Av. Revolución 1500, CP 44420 Guadalajara, Jalisco, Mexico
e-mail: nesterov@cencar.udg.mx

J. M. Sánchez Martínez
e-mail: jmsm.manuel@gmail.com

G. P. Berman
Theoretical Division, Los Alamos National Laboratory, Los Alamos, NM 87544, USA
e-mail: gpb@lanl.gov

R. T. Sayre
Los Alamos National Laboratory and New Mexico Consortium, 4200 W James Rd, Los Alamos, NM 87544, USA
e-mail: rsayre@newmexicoconsortium.org

Keywords Non-Hermitian Hamiltonian · Photosynthetic complexes · Electron transfer · Noise · Sink

1 Introduction

In photosynthetic complexes of plants, eukaryotic algae and cyanobacteria, quanta of light excite chlorophyll dipoles in the antennas of the light harvesting complexes (LHCs). These local energy excitations are then transferred to the reaction centers (RCs) of photosystem I (PSI) and photosystem II (PSII), where the charge separation occurs. During charge separation an electron jumps from the donor to the acceptor and both donor and acceptor become charged. These electron jumps continue through out the whole chain of the redox potential. The characteristic time-scales of the electron dynamics vary from a few picoseconds to milliseconds. The primary charge separation occurs on a very short time-scale, of a few picoseconds [1–5]. Because this time-scale is so short, even the room-temperature fluctuations of the protein environment do not destroy the quantum coherent effects, which were recently discussed in LHCs and RCs [5–12].

Generally, to describe the motion of an electron between the donor and acceptor, different approaches can be used [5,7,13–23]. The leading approach is based on the well-known Marcus theory, which takes into account both the strength of donor-acceptor interaction, and the dynamics of the protein environment [15]. In this way, the election transfer (ET) rate and the efficiency of the ET can be calculated. At the same time, many efforts have been devoted to various modifications of the Markus theory. One of them is related to taking into account the sinks which represent the continuum electron energy reservoirs in the chemical and biological systems [13,14, 24] (see also references therein). These continuum manifolds are similar to those described by the Weisskopf–Wigner model and its different modifications [25–27]. These sink reservoirs serve as additions to the thermal reservoirs in ET. The principal difference between the protein (vibrational) and sink (electron) reservoirs is that the former behave as the bosonic (electromagnetic) environments while the later provide additional electron quasi-degenerate states [25,26]. These sinks increase the entropy for an electron escaping into these reservoirs. As a result, the sinks modify the form of the Gibbs equilibrium distribution. Indeed, even in the case of a flat redox potential one can expect the acceptor to be populated with a high enough efficiency.

In this paper, we consider ET in a model which consists of two discrete energy states, donor and acceptor. A matrix element of a direct donor-acceptor interaction is included. The donor and acceptor interact directly with two independent sinks which are represented by two quasi-degenerate (continuum) manifolds of the electron energy levels. In addition, external (classical) noise interacts with both donor and acceptor. By taking into account all these effects, we describe the ET dynamics in different parameter regions. We obtain the conditions when the system of integro-differential equations, which describes generally the non-Markovian electron dynamics, can be reduced to much simpler system of ordinary differential equations. We obtain analytically and numerically the ET for both sharp and flat redox potentials, and for different amplitudes of noise.

The advantageous of our approach include (i) simultaneous consideration of the standard donor-acceptor interaction, interactions with sinks, and with external noise and (ii) a derivation of explicit analytical expressions which could be useful for the analysis of the ET in these systems. Our approach is a rigorous one, so all approximations are controlled and justified. Simultaneous contributions of sinks and noise allowed us to derive optimal ET rates for various regions of parameters. In particular, we demonstrate that even for flat redox potential, the efficiency of the population of acceptor can be high enough. As was mentioned above, we substituted in our model the thermodynamical (protein) environment by the external classical noise (see, for example, [22,28–31]). We discuss a relation between our approach and the Marcus theory of ET.

Our paper is organized as follows. In Sect. 2, we describe our simplified model with a single sink interacting only with the acceptor level, and present an analytic solution for the ET, in the absence of noise. In Sect. 3, we analyze analytically and numerically the simultaneous influence of the single acceptor sink and noise. We derive a closed system of integro-differential equations which describe the ET. We also find the region of parameters for which a system of ordinary differential equations can be applied. In Sect. 4, we analyze analytically and numerically the simultaneous influence of two sinks and noise. In Sect. 5, we discuss the obtained results. In the Appendices some useful formulae are presented.

2 Model description

Our model consists of two protein cofactors in the RC (donor and acceptor) each with a discrete energy level. In this Section, we consider, for simplicity, only a single sink which interacts with the acceptor level (the acceptor is embedded in a sink). The sink can be considered either as an additional, third cofactor, or as a part of the acceptor (see Fig. 1). The first site, denoted by $|d\rangle$, is the electron donor, with the energy level, E_d. The second site, $|a\rangle$, is the electron acceptor, with energy level, E_a. We model the sink by a large number of discrete and nearly degenerate energy levels, $N_a \gg 1$ (Fig. 1). Then, the transition to the density of states (the continuum limit) is done for the sink. Note that in some situations, the sinks can be considered as approximations to HOMO and LUMO orbitals with finite electron densities of states.

The Hamiltonian of this system can be written as

$$H_t = E_d|d\rangle\langle d| + E_a|a\rangle\langle a| + \frac{V}{2}(|d\rangle\langle a| + |a\rangle\langle d|) + \sum_{i=1}^{N} E_i|i\rangle\langle i| + \sum_{i=1}^{N_a}(V_{ai}|a\rangle\langle i| + V_{ia}|i\rangle\langle a|)\,, \tag{1}$$

where E_i are energies of the sink levels, and $V_{da} = V/2$ (see Fig. 1).

Using the standard Feshbach projection method [26,32–35], one can show that the dynamics of the donor-acceptor (intrinsic) states can be described by the following Schrödinger equation with an effective non-Hermitian Hamiltonian, $\tilde{\mathscr{H}} = \mathscr{H} - i\mathscr{W}$

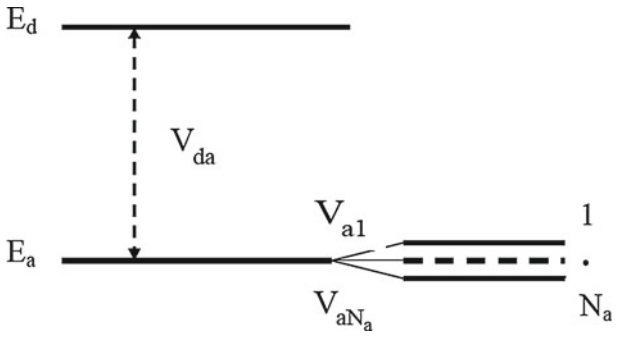

Fig. 1 Schematic of our model consisting of donor and acceptor discrete energy levels, with the acceptor coupled to a sink reservoir with a nearly continuous spectrum

(we set $\hbar = 1$)[36]:

$$i\frac{\partial\psi(t)}{\partial t} = \tilde{\mathscr{H}}\psi(t), \tag{2}$$

where

$$\mathscr{H} = \varepsilon_d|d\rangle\langle d| + \varepsilon_a|a\rangle\langle a| + \frac{V}{2}(|d\rangle\langle a| + |a\rangle\langle d|) \tag{3}$$

is the dressed donor-acceptor Hamiltonian, and $\mathscr{W} = (\Gamma_a/2)|a\rangle\langle a|$. Here Γ_a is the rate describing the tunneling from the acceptor to the sink. (See Appendix A for details.)

Equivalently, the dynamics of this system can be described by the Liouville equation,

$$i\dot{\rho} = [\mathscr{H}, \rho] - i\{\mathscr{W}, \rho\}, \tag{4}$$

where ρ is the density matrix projected on the intrinsic states, and $\{\mathscr{W}, \rho\} = \mathscr{W}\rho + \rho\mathscr{W}$.

The solution of the eigenvalue problem for the effective non-Hermitian Hamiltonian, $\tilde{\mathscr{H}}$, yields two complex eigenvalues:

$$\tilde{E}_{1,2} = \frac{1}{2}(\varepsilon_d + \varepsilon_a - i\Gamma) \pm \frac{\Omega}{2} \tag{5}$$

where $\Omega = \sqrt{V^2 + (\varepsilon_{da} + i\Gamma)^2}$, $\Gamma = \Gamma_a/2$ and we denote $\varepsilon_{da} = \varepsilon_d - \varepsilon_a$. The eigenvalues coalescence in the so-called exceptional point (EP) defined by the equation, $\Omega(V, \varepsilon_{da}, \Gamma) = 0$. Since Ω is a complex function of its parameters, we obtain two real equations: $\Re\Omega = 0$ and $\Im\Omega = 0$. One can show that these equations are equivalent to $\varepsilon_{da} = 0$ and $V = \Gamma$.

Note that, in contrast to the case of a Hermitian Hamiltonian, where the degeneracy is referred to as a "conical intersection" (known also as a "diabolic point" [37]), the

coalescence of eigenvalues results in different eigenvectors. At the EP, the eigenvectors merge, forming a Jordan block. (See the review [38], and references therein.)

Choice of parameters. This model involves various parameters, whose values are only partially known. Our choice of parameters is based on the data taken for the ET through the active pathway in the quinone-type of the Photosystem II RC [39]. (Note that the values of parameters in energy units can be obtained by multiplying our values by $\hbar \approx 6.58 \times 10^{-13}$meVs. For example, $\varepsilon_{da} = 60\ \mathrm{ps}^{-1} \approx 40$meV.)

2.1 Tunneling to the sink

In this section we discuss the ET to the sink. (For details see [36].) We assume that initially the electron occupies the upper level (donor), $\rho_{11}(0) = 1$ and $\rho_{22}(0) = 0$. With these initial conditions, the solution of the Liouville equation (4) for the diagonal component of the density matrix is:

$$\rho_{11}(t) = e^{-\Gamma t} \left| \left(\cos \frac{\Omega t}{2} - i \cos\theta \sin \frac{\Omega t}{2} \right) \right|^2, \tag{6}$$

$$\rho_{22}(t) = e^{-\Gamma t} \left| \sin\theta \sin \frac{\Omega t}{2} \right|^2, \tag{7}$$

where $\Omega = \sqrt{V^2 + (\varepsilon_{da} + i\Gamma)^2}$ is the complex Rabi frequency, $\cos\theta = (\varepsilon_{da} + i\Gamma)/\Omega$, and $\sin\theta = V/\Omega$.

Setting $\Omega = \Omega_1 + i\Omega_2 = \sqrt{p + iq}$, where $p = V^2 + \varepsilon_{da}^2 - \Gamma^2$ and $q = 2\varepsilon_{da}\Gamma$, we obtain

$$\Omega_1 = \pm \frac{1}{\sqrt{2}} \sqrt{p + \sqrt{p^2 + q^2}}, \tag{8}$$

$$\Omega_2 = \pm \frac{1}{\sqrt{2}} \sqrt{-p + \sqrt{p^2 + q^2}}. \tag{9}$$

Using these results, we obtain for $\rho_{22}(t)$ the simple analytical expression:

$$\rho_{22}(t) = \frac{V^2 e^{-\Gamma t}}{2(\Omega_1^2 + \Omega_2^2)} \left(\cosh \Omega_2 t - \cos \Omega_1 t \right). \tag{10}$$

We define the ET efficiency of tunneling to the sink as

$$\eta(t) = 1 - \mathrm{Tr}(\rho(t)) = \int_0^t \mathrm{Tr}\{\mathscr{W}, \rho(\tau)\} d\tau. \tag{11}$$

This can be recast as the integrated probability of trapping the electron in the sink [11,40],

$$\eta(t) = 2\Gamma \int_0^t \rho_{22}(\tau) d\tau. \tag{12}$$

Inserting $\rho_{22}(t)$ into (12) and performing the integration, we find that the ET efficiency is given by

$$\eta(t) = 1 - \frac{e^{-\Gamma t}}{\Gamma(\Omega_1^2 + \Omega_2^2)} \Big((\Gamma^2 + \Omega_1^2)(\Gamma \cosh \Omega_2 t + \Omega_2 \sinh \Omega_2 t) \\ -(\Gamma^2 - \Omega_2^2)(\Gamma \cos \Omega_1 t - \Omega_1 \sin \Omega_1 t) \Big). \tag{13}$$

In [36] it was shown that, for the sharp redox potential, the ET efficiency is rather slow function of time. For instance, for $\varepsilon_{da} = 60\,\mathrm{ps}^{-1}$ and $10\,\mathrm{ps} < \mathrm{V} < 40\,\mathrm{ps}^{-1}$, the ET efficiency approaches a value close to 1 for relatively large times, $t \gtrsim 150$ ps. However, the situation is changes drastically for the flat redox potential. For example, for $\varepsilon_{da} = 0$, we obtain

$$\begin{array}{ll} \Omega_2 = 0, \ \Omega_1^2 = V^2 - \Gamma^2, & V > \Gamma, \\ \Omega_1 = 0, \ \Omega_2 = 0, & V = \Gamma \\ \Omega_1 = 0, \ \Omega_2^2 = \Gamma^2 - V^2, & \Gamma > V. \end{array} \tag{14}$$

Using these relations, we find that at the exceptional point the ET efficiency behaves as

$$\eta(t) = 1 - e^{-\Gamma t}. \tag{15}$$

For $V \ll \Gamma$ ($V \gg \Gamma$) the asymptotic behavior of $\eta(t)$ is

$$\eta(t) \sim \begin{cases} 1 - e^{-\Gamma t}, & V \gg \Gamma, \\ 1 - e^{-V^2 t/2\Gamma}, & V \ll \Gamma. \end{cases} \tag{16}$$

Comparing the obtained results with (13), we conclude that the highest ET rate is obtained for the flat redox potential at $\varepsilon_{da} = 0$, and $V \geq \Gamma$. This result can be interpreted by using a model of a single spin dynamics in an effective magnetic field. The above parameters are defined so that the effective magnetic field is oriented in the positive x-direction, and V corresponds to the Rabi frequency–the frequency of rotation of the spin around the x-axis. Then, the above chosen conditions provide a rapid transition from the donor to the acceptor, with subsequent tunneling from the acceptor to the sink. The results of numerical simulations of the ET efficiency are presented in Fig. 2. One can see that, when $\varepsilon_{da} = 0$ and $V \geq \Gamma$, the ET efficiency can approach a value close to 1 for short enough times, ~ 2 ps.

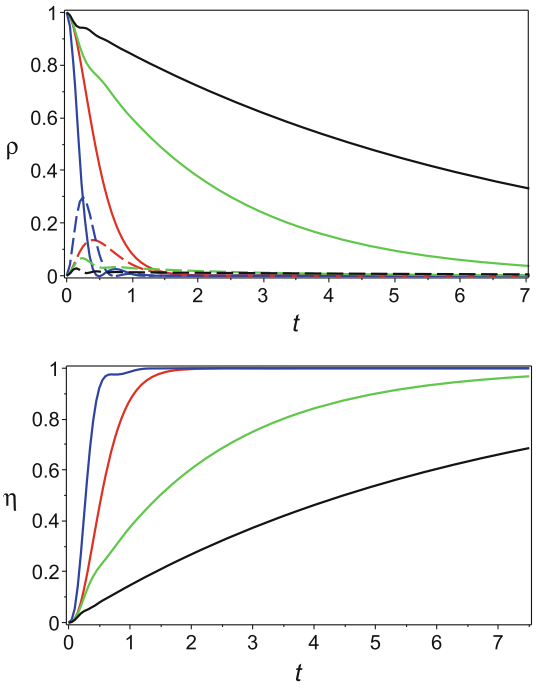

Fig. 2 (Color online) Time dependence (in ps) of the sites population, $\rho_{11}(t)$ and $\rho_{22}(t)$, (*top*) and ET efficiency (*bottom*) ($\Gamma = 5\,\mathrm{ps}^{-1}$). *Solid* and *dashed lines* correspond to, $\rho_{11}(t)$ and $\rho_{22}(t)$, respectively. *Blue line*: $V = 10\,\mathrm{ps}^{-1}$, $\varepsilon_{da} = 0$; *red line* (EP): $V = \Gamma = 5\,\mathrm{ps}^{-1}$, $\varepsilon_{da} = 0$; *green line*: $V = 10\,\mathrm{ps}^{-1}$, $\varepsilon_{da} = 10\,\mathrm{ps}^{-1}$; *black line*: $V = 5\,\mathrm{ps}^{-1}$, $\varepsilon_{da} = 20\,\mathrm{ps}^{-1}$

3 Noise-assisted electron transfer to the sink

In the presence of classical noise, the quantum dynamics of the ET can be described by the following effective non-Hermitian Hamiltonian (for details see Appendix A):

$$\tilde{\mathscr{H}} = \sum_n \varepsilon_n |n\rangle\langle n| + \sum_{m,n} \lambda_{mn}(t)|m\rangle\langle n| + \frac{V}{2}\sum_{m\neq n}|m\rangle\langle n| - i\frac{\Gamma_2}{2}|2\rangle\langle 2|, \quad m,n = 1,2, \tag{17}$$

where $\lambda_{mn}(t)$ describes the noise. We denote by $|1\rangle$ and $|2\rangle$ the donor and acceptor states in the site representation, respectively. The diagonal matrix elements of noise, λ_{nn}, are responsible for decoherence, and the off-diagonal matrix elements, λ_{mn} ($m \neq n$), lead to the relaxation processes. In what follows, we use a spin-fluctuator model of noise, modeling the noise by an ensemble of fluctuators [41–43].

In the rest of this paper, we restrict ourselves to considering only the diagonal noise effects, assuming that the noisy environment is the same for both the donor and the acceptor sites (collective noise). Then, one can write $\lambda_1(t) = g_1\xi(t)$ and $\lambda_2(t) = g_2\xi(t)$, where $g_{1,2}$ are the interaction constants, and we assume, for concreteness, that $g_1 \leq g_2$. We consider a stationary noise described by a random variable, $\xi(t)$, so that

$$\xi_0 = \langle\xi(t)\rangle = \langle\xi(0)\rangle, \tag{18}$$

$$\chi(t-t') = \langle \xi(t)\xi(t') \rangle, \tag{19}$$

where $\chi(t-t')$ is the correlation function.

The evolution of the average diagonal components of the density matrix is described by the following system of integro-differential equations (see Appendix B):

$$\frac{d}{dt}\langle \rho_{11}(t) \rangle = -\int_0^t K(t,t') \left(\langle \rho_{11}(t') \rangle - \langle \rho_{22}(t') \rangle \right) dt', \tag{20}$$

$$\frac{d}{dt}\langle \rho_{22}(t) \rangle = \int_0^t K(t,t') \left(\langle \rho_{11}(t') \rangle - \langle \rho_{22}(t') \rangle \right) dt' - 2\Gamma \langle \rho_{22}(t) \rangle, \tag{21}$$

where the average $\langle\ \rangle$ is taken over the random process describing noise, and the kernel, $K(t,t')$, is given by

$$K(t,t') = e^{-\Gamma(t-t')} \left(\left\langle \tilde{V}_{21}(t)\tilde{V}_{12}(t') \right\rangle + \left\langle \tilde{V}_{21}(t')\tilde{V}_{12}(t) \right\rangle \right). \tag{22}$$

We obtain the following expression for the kernel:

$$K(t-t') = \frac{V^2}{2} \cos\left(\varepsilon(t-t')\right) \exp\left(-\Gamma(t-t') - D^2 \int_0^{t-t'} d\tau' \int_0^{\tau'} d\tau'' \chi(\tau'-\tau'') \right), \tag{23}$$

where $D = |g_1 - g_2|$, $\varepsilon = \varepsilon_{da} - \lambda_0$, and we denote $\lambda_0 = D\xi_0$.

In our numerical simulations we use the correlation function of noise introduced in [43],

$$\chi(\tau) = \sigma^2 A \left(E_1(2\gamma_m \tau) - E_1(2\gamma_c \tau) \right), \quad \tau = |t-t'|. \tag{24}$$

Here $E_n(z)$ denotes the Exponential integral [44], $A = 1/\ln(\gamma_c/\gamma_m)$, $\sigma^2 = \chi(0)$ and γ_m and γ_c ($\gamma_m \ll \gamma_c$) indicate the boundaries of the switching rates in the ensemble of random fluctuators. The correlation function includes, besides the amplitude, σ, two fitting parameters: γ_m and γ_c. Taking into account available theoretical and experimental data [30,45,46], we have chosen for our numerical simulations the parameters γ_m and γ_c as follows: $2\gamma_m = 10^{-4}\text{ps}^{-1}$, $2\gamma_c = 1\text{ps}^{-1}$.

In Figs. 3 and 4 we present the results of numerical simulations for the tunneling rate, $\Gamma = 1\,\text{ps}^{-1}$, and different parameters, V, ε, and the amplitude of noise, $D\sigma$. As one can see from Fig. 3, a low level of the noise does not improve the ET efficiency rates. However, if the amplitude is sufficiently large, the noise significantly accelerates the ET to the sink (Fig. 4).

In [36] we show that for a sharp redox potential, noise can greatly improve the rate of ET to the sink. Our numerical results presented in Fig. 4, demonstrate that this is

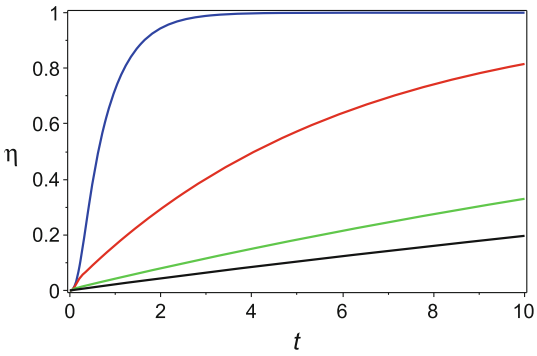

Fig. 3 (Color online) Time dependence (ps) of the ET efficiency ($V = \Gamma = 1\,\mathrm{ps}^{-1},\ D\sigma = 5\,\mathrm{ps}^{-1}$). *Blue line*: $\varepsilon = 0$ (EP), *red line*: $\varepsilon = 20\,\mathrm{ps}^{-1}$, *green line*: $\varepsilon = 40\,\mathrm{ps}^{-1}$, *black line*: $\varepsilon = 60\,\mathrm{ps}^{-1}$

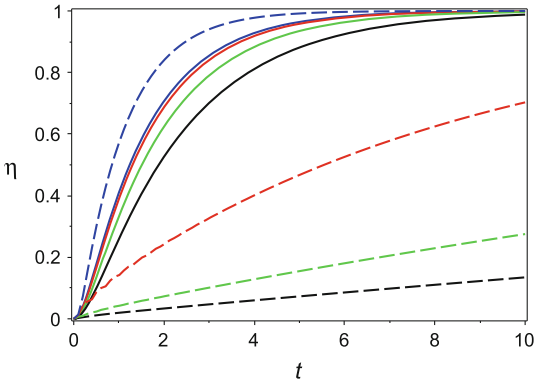

Fig. 4 (Color online) Time dependence (in ps) of the ET efficiency ($V = 10\,\mathrm{ps}^{-1},\ \Gamma = 1\,\mathrm{ps}^{-1}$). *Solid lines* correspond to $\eta(t)$ in the presence of noise with the amplitude $D\sigma = 40\,\mathrm{ps}^{-1}$. *Blue line*: $\varepsilon = 0$, *red line*: $\varepsilon = 20\,\mathrm{ps}^{-1}$, *green line*: $\varepsilon = 40\,\mathrm{ps}^{-1}$, *black line*: $\varepsilon = 60\,\mathrm{ps}^{-1}$. *Dashed lines* correspond to $\eta(t)$, in the absence of noise

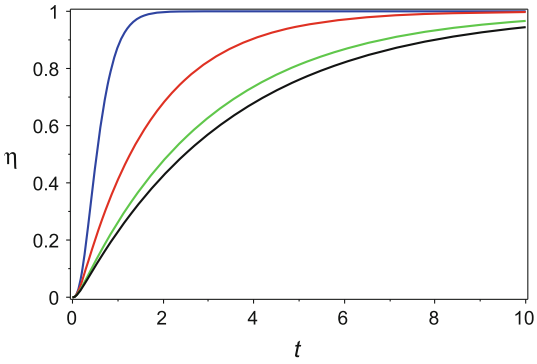

Fig. 5 (Color online) Time dependence (in ps) of the ET efficiency at the EP in the presence of noise ($\varepsilon = 0,\ V = \Gamma = 5\,\mathrm{ps}^{-1}$). *Blue line*: $D\sigma = 0$, *red line*: $D\sigma = 20\,\mathrm{ps}^{-1}$, *green line*: $D\sigma = 40\,\mathrm{ps}^{-1}$, *black line*: $D\sigma = 60\,\mathrm{ps}^{-1}$

true for any redox potential, if the noise is strong enough. In Fig. 5 we present the results of numerical simulations at the EP and in presence of noise for the tunneling rate $\Gamma = 5\,\mathrm{ps}^{-1}$ ($\varepsilon = 0,\ V = \Gamma = 5\,\mathrm{ps}^{-1}$). As can be observed, at the exceptional point (EP) the noise decreases the rate of the ET. The behavior of the system in the vicinity of the EP is rather complicated, and the ET efficiency is sensitive to the choice of parameters (Fig. 6). For instance, for the flat redox potential with $\varepsilon = 0$ and an

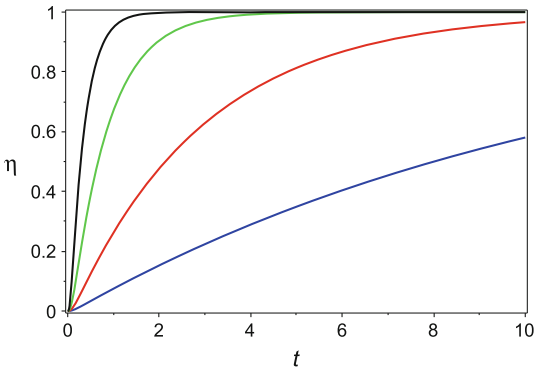

Fig. 6 (Color online) Time dependence (in ps) of the ET efficiency in the vicinity of the EP in the presence of noise ($\varepsilon = 0$, $D\sigma = 60\,\mathrm{ps}^{-1}$, $\Gamma = 5\,\mathrm{ps}^{-1}$). *Blue line*: $V = 2.5\,\mathrm{ps}^{-1}$, *red line*: $V = 5\,\mathrm{ps}^{-1}$ (EP), *green line*: $V = 10\,\mathrm{ps}^{-1}$, *black line*: $V = 20\,\mathrm{ps}^{-1}$

amplitude of noise, $D\sigma = 60\,\mathrm{ps}^{-1}$, the ET efficiency approaches a value close to 1 for short enough time, ~ 2 ps.

3.1 Electron transport approximated by differential equations

Under the conditions, presented below, the system of integro-differential Eqs. (20) and (21), can be approximated by the following system of the ordinary differential equations:

$$\frac{d}{dt}\langle\rho_{11}(t)\rangle = -\Re(t)\left(\langle\rho_{11}(t)\rangle - \langle\rho_{22}(t)\rangle\right), \tag{25}$$

$$\frac{d}{dt}\langle\rho_{22}(t)\rangle = \Re(t)\left(\langle\rho_{11}(t)\rangle - \langle\rho_{22}(t)\rangle\right) - 2\Gamma\langle\rho_{22}(t)\rangle, \tag{26}$$

$$\frac{d}{dt}\eta(t) = 2\Gamma\langle\rho_{22}(\tau)\rangle, \tag{27}$$

where $\Re(t) = \int_0^t K(\tau)d\tau$ and $\eta(t) = 2\Gamma\int_0^t\langle\rho_{22}(\tau)\rangle d\tau$.

Now we obtain the conditions for which the exact system of integro-differential Eqs. (20) and (21) can be approximated by Eqs. (25)–(27). In the first order of the series expansion, we can write

$$\langle\rho_{11}(t')\rangle \approx \langle\rho_{11}(t)\rangle - \frac{d}{dt}\langle\rho_{11}(t)\rangle(t-t'), \tag{28}$$

$$\langle\rho_{22}(t')\rangle \approx \langle\rho_{22}(t)\rangle - \frac{d}{dt}\langle\rho_{22}(t)\rangle(t-t'), \tag{29}$$

where, in the same order, the derivatives on the r.h.s. are taken from Eqs. (25), (27).

Using these results, after some transformations we find that Eqs. (20) and (21) become

$$\frac{d}{dt}\langle\rho_{11}(t)\rangle = -\Re(t)\left(\langle\rho_{11}(t)\rangle - \langle\rho_{22}(t)\rangle\right)\left(1-\Re_1(t)\right) + 2\Gamma\Re_1(t)\langle\rho_{22}(t)\rangle, \tag{30}$$

$$\frac{d}{dt}\langle\rho_{22}(t)\rangle = \Re(t)\left(\langle\rho_{11}(t)\rangle - \langle\rho_{22}(t)\rangle\right)(1-\Re_1(t)) - 2\Gamma\langle\rho_{22}(t)\rangle(1-\Re_1(t)), \tag{31}$$

$$\frac{d}{dt}\eta(t) = 2\Gamma\langle\rho_{22}(\tau)\rangle, \tag{32}$$

where $\Re_1(t) = \int_0^t \tau K(\tau)d\tau$. From here it follows that the system of integro-differential Eqs. (20) and (21) can be approximated by the system of the first order ordinary differential equations in the interval of time: $0 < t < \infty$, if $|\int_0^\infty \tau K(\tau)d\tau| \ll 1$.

Assuming that the correlation function, $\chi(t)$, is a rapidly decreasing function, as $t \to \infty$, we can approximate

$$\exp\left(-D^2\int_0^t d\tau\int_0^\tau ds\,\chi(\tau-s)\right) \approx \exp\left(-\frac{(D\sigma t)^2}{2}\right). \tag{33}$$

Performing the integration with the kernel

$$K(\tau) = \frac{V^2}{2}\cos(\varepsilon\tau)\exp\left(-\Gamma\tau - \frac{(D\sigma)^2}{2}\tau^2\right), \tag{34}$$

we obtain the following estimate:

$$\left|\int_0^\infty K(\tau)\tau d\tau\right| = \left|\frac{V^2\delta}{2D^2\sigma^2}\right| < \frac{V^2|\delta|_{\max}}{2D^2\sigma^2} \ll 1, \tag{35}$$

where

$$\delta = -1 + \frac{\sqrt{\pi}q}{4p}\exp\left(\frac{q^2}{4p^2}\right)\operatorname{erfc}\left(\frac{q}{2p}\right) + \frac{\sqrt{\pi}\bar{q}}{4p}\exp\left(\frac{\bar{q}^2}{4p^2}\right)\operatorname{erfc}\left(\frac{\bar{q}}{2p}\right). \tag{36}$$

Here $p = D\sigma/\sqrt{2}$, $q = \Gamma + i\varepsilon$, $\bar{q} = \Gamma - i\varepsilon$, and $\operatorname{erfc}(z)$ denotes the complementary error function [44].

Using the properties of the erfc function, one can show that $|\delta| \le 1$ for any choice of parameters Γ, ε and the amplitude of noise, $D\sigma$. (See Fig. 7.) Consequently, the condition of validity of the approximation (25)–(27) can be written as $V \ll D\sigma$. This rough estimate can be improved greatly for the high level of noise, leading to $V \le D\sigma$.

In Figs. 8 and 9 we present the results of the numerical simulations for ET efficiency,

$$\eta(t) = 2\Gamma\int_0^t \langle\rho_{22}(\tau)\rangle d\tau. \tag{37}$$

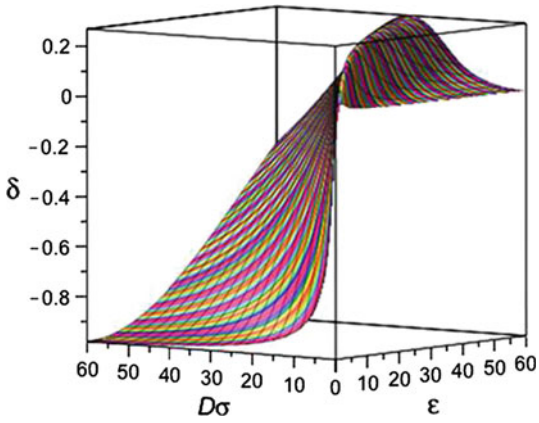

Fig. 7 (Color online) Dependence of δ on ε and $D\sigma$ ($\Gamma = 1\,\mathrm{ps}^{-1}$)

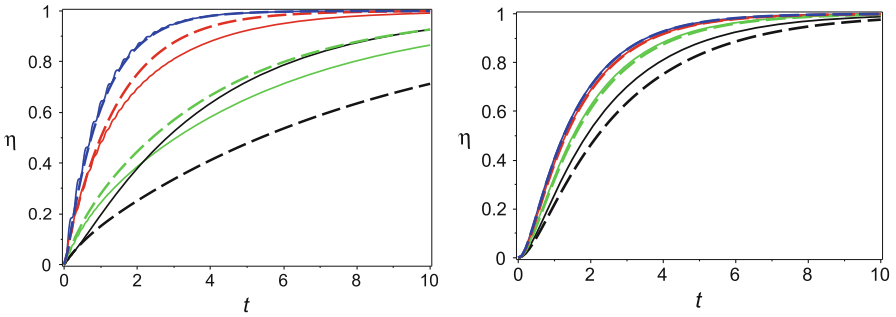

Fig. 8 (Color online) Time dependence (in ps) of the ET efficiency, $\eta(t)$. The solutions of the system of integro-differential equations are presented by *solid lines* ($\Gamma = 1\,\mathrm{ps}^{-1}$). *Dashed lines* correspond to the solutions of the approximate system of differential equations. *Blue line*: $\varepsilon = 0$, *red line*: $\varepsilon = 20\,\mathrm{ps}^{-1}$, *green line*: $\varepsilon = 40\,\mathrm{ps}^{-1}$, *black line*: $\varepsilon = 60\,\mathrm{ps}^{-1}$. *Top*: $V = 30\,\mathrm{ps}^{-1}$, $D\sigma = 5\,\mathrm{ps}^{-1}$. *Bottom*: $V = 10\,\mathrm{ps}^{-1}$, $D\sigma = 40\,\mathrm{ps}^{-1}$

As one can see, for $V \leq D\sigma$ there is good agreement between the solutions obtained from the system of integro-differential Eqs. (20) and (21) and the approximate system of differential Eqs. (25)–(27).

The advantage of using differential equations instead of integro-differential equations is the ability to introduce effective rates. The computation of the asymptotic rate, $\Re_\Gamma = \lim_{t\to\infty} \Re(t)$, yields [36]

$$\Re_\Gamma = \frac{V^2\sqrt{2\pi}}{8D\sigma}\left(\exp\left(\frac{(\Gamma+i\varepsilon)^2}{2D^2\sigma^2}\right)\mathrm{erfc}\left(\frac{\Gamma+i\varepsilon}{\sqrt{2}D\sigma}\right) + \exp\left(\frac{(\Gamma-i\varepsilon)^2}{2D^2\sigma^2}\right)\mathrm{erfc}\left(\frac{\Gamma-i\varepsilon}{\sqrt{2}D\sigma}\right)\right). \tag{38}$$

As one can see from Fig. 10, for given values, V and ε, the rate, $\Re_\Gamma$, reaches its maximum value when the amplitude of noise equals the energy difference between donor and acceptor, $D\sigma \approx \varepsilon$.

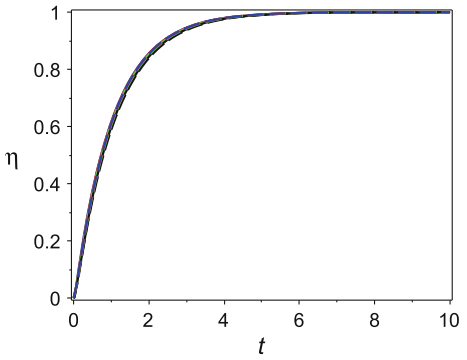

Fig. 9 (Color online) Time dependence (in ps) of the ET efficiency. *Solid lines* correspond to $\eta(t)$ obtained from the system of integro-differential Eqs. (20)–(21) and *dashed lines* present the results for $\eta(t)$ obtained from the system of differential Eqs. (25)–(27). *Blue line*: $\varepsilon = 0$, *red line*: $\varepsilon = 20\,\mathrm{ps}^{-1}$, *green line*: $\varepsilon = 40\,\mathrm{ps}^{-1}$, *black line*: $\varepsilon = 60\,\mathrm{ps}^{-1}$ ($\Gamma = 1\,\mathrm{ps}^{-1}$, $V = D\sigma = 40\,\mathrm{ps}^{-1}$). One can observe the excellent agreement between the solutions

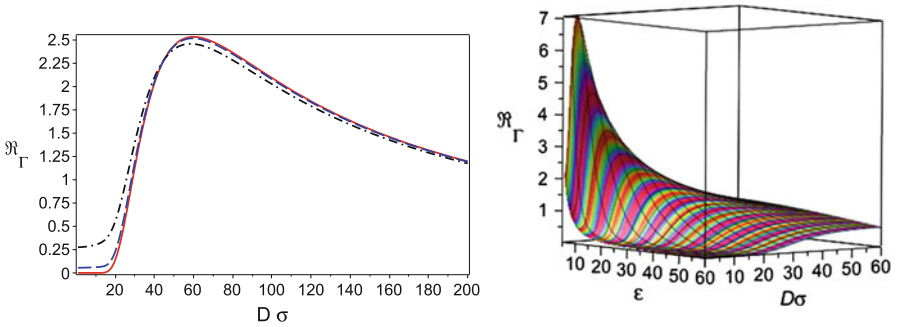

Fig. 10 (Color online) *Left panel*. The ET asymptotic rate, $\Re_\Gamma$, vs. the amplitude of noise, $D\sigma$ ($\varepsilon = 60\,\mathrm{ps}^{-1}$, $V = 20\,\mathrm{ps}^{-1}$). *Black dash-dot line* ($\Gamma = 5\,\mathrm{ps}^{-1}$), *blue dashed line* ($\Gamma = 1\,\mathrm{ps}^{-1}$), *red solid line* ($\Gamma = 0$). *Right panel*. Dependence of the asymptotic rate, $\Re_\Gamma$, on ε and $D\sigma$ ($V = 10\,\mathrm{ps}^{-1}$, $\Gamma = 1\,\mathrm{ps}^{-1}$)

We compare now our results with the predictions of the Marcus theory, which gives for the ET rate [15,19,20],

$$\Re = \frac{V^2}{4}\sqrt{\frac{\pi}{\lambda k_B T}}\exp\left(-\frac{(\varepsilon_{da}-\lambda)^2}{4\lambda k_B T}\right), \tag{39}$$

where λ is the reorganization energy, and T is temperature. As in Marcus theory the sink is absent, we insert $\Gamma = 0$ into Eq. (38). We obtain for our case,

$$\Re_0 = \frac{V^2}{4}\sqrt{\frac{2\pi}{D^2\sigma^2}}\exp\left(-\frac{(\varepsilon_{da}-\lambda_0)^2}{2D^2\sigma^2}\right). \tag{40}$$

The functional form of the rate (40) agrees with the ET rate followed from the Marcus theory if one identifies: $\lambda_0 = \lambda$ and $D^2\sigma^2 = 2\lambda k_B T$.

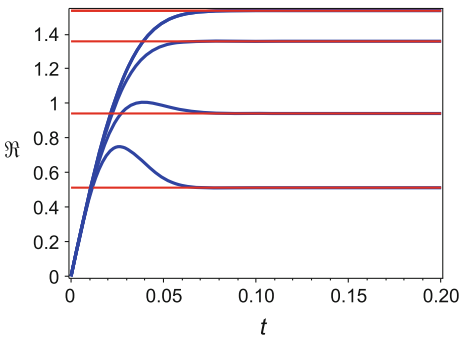

Fig. 11 (Color online) *Blue line* describes the time dependence of the ET rate, $\Re(t)$. *Red line* corresponds to the asymptotic rate, $\Re_\Gamma$, given by Eq. (38). From *top* to *bottom*: $\varepsilon = 0,\ 20,\ 40,\ 60\,\mathrm{ps}^{-1}$ ($\Gamma = 1\,\mathrm{ps}^{-1}$, $V = 10\,\mathrm{ps}^{-1}$ and $D\sigma = 40\,\mathrm{ps}^{-1}$)

In Fig. 11, we compare the results of numerical calculations of the relaxation rate, $\Re(t)$ (blue line), with the asymptotic expression $\Re_\Gamma$ (red line) for different choices of parameters. Inserting $\Re_\Gamma$ instead of $\Re(t)$ into Eqs. (25) and (26), we obtain the following system of the differential equations:

$$\frac{d}{dt}\langle\rho_{11}(t)\rangle = -\Re_\Gamma\left(\langle\rho_{11}(t)\rangle - \langle\rho_{22}(t)\rangle\right), \tag{41}$$

$$\frac{d}{dt}\langle\rho_{22}(t)\rangle = \Re_\Gamma\left(\langle\rho_{11}(t)\rangle - \langle\rho_{22}(t)\rangle\right) - 2\Gamma\langle\rho_{22}(t)\rangle. \tag{42}$$

The solution is given by

$$\langle\rho_{11}(t)\rangle = \left(\frac{1}{2} - \frac{\Gamma}{2\sqrt{\Re_\Gamma^2 + \Gamma^2}}\right)e^{-\Re_1 t} + \left(\frac{1}{2} + \frac{\Gamma}{2\sqrt{\Re_\Gamma^2 + \Gamma^2}}\right)e^{-\Re_2 t}, \tag{43}$$

$$\langle\rho_{22}(t)\rangle = \frac{\Re_\Gamma}{2\sqrt{\Re_\Gamma^2 + \Gamma^2}}\left(e^{-\Re_2 t} - e^{-\Re_1 t}\right), \tag{44}$$

where $\Re_{1,2} = \Re_\Gamma + \Gamma \pm \sqrt{\Re_\Gamma^2 + \Gamma^2}$. The computation of the ET efficiency yields [36]

$$\eta(t) = 1 - e^{-\frac{(\Re_1+\Re_2)t}{2}}\left(\cosh\frac{(\Re_1 - \Re_2)t}{2} + \frac{\Re_1 + \Re_2}{\Re_1 - \Re_2}\sinh\frac{(\Re_1 - \Re_2)t}{2}\right). \tag{45}$$

Its asymptotic behavior is

$$\eta(t) \approx 1 - \frac{\Re_1}{\Re_1 - \Re_2}e^{-\Re_2 t}. \tag{46}$$

As one can see from Eq. (45), there are two ET rates, $\Re_1$ and $\Re_2$. However, the asymptotic behavior of the ET efficiency is defined by the lowest ET rate, $\Re_2$.

As shown in Fig. 11, the ET rate reaches its asymptotic value, $\Re(t) \to \Re_\Gamma$, quite rapidly, at $t \approx 0.1$ ps. This allows us to use the analytical solutions to describe tunneling

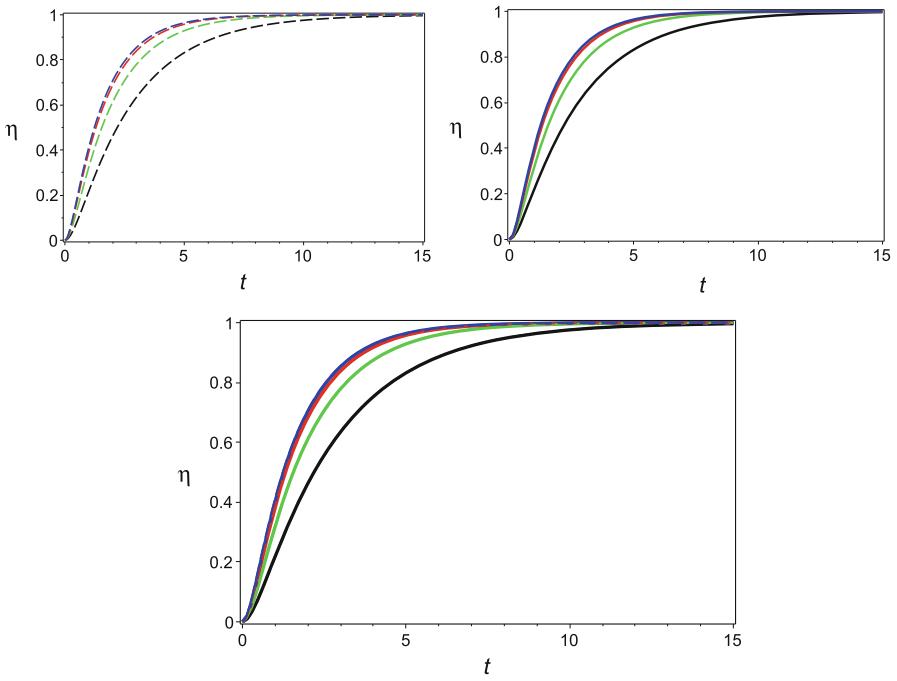

Fig. 12 (Color online) Time dependence (in ps) of the ET efficiency, $\eta(t)$ ($\Gamma = 1\,\mathrm{ps}^{-1}$, $V = 10\,\mathrm{ps}^{-1}$, $D\sigma = 40\,\mathrm{ps}^{-1}$). *Top. Left*: analytical solution (*dashed lines*). *Right*: results of numerical simulations (*solid lines*). *Blue line*: $\varepsilon = 0$, *red line*: $\varepsilon = 20\,\mathrm{ps}^{-1}$, *green line*: $\varepsilon = 40\,\mathrm{ps}^{-1}$, *black line*: $\varepsilon = 60\,\mathrm{ps}^{-1}$. *Bottom*. The both graphics are overlapping

to the sink with very high degree of accuracy. This conclusion is confirmed by our numerical simulations presented in Fig. 12. One can observe the excellent agreement between the ET efficiency given by formula (45) and the results obtained from Eqs. (25)–(27).

4 Modified model with two sinks

In this Section, we generalize our model by including two sinks interacting independently with the donor and acceptor. (See Fig. 13). The main reasons for this generalization are the following. When using a single sink which interacts with the acceptor, the asymptotic of the ET efficiency, $\eta(t)$, for large times approaches unity independently of the parameters of the system and the tunneling rate, Γ. The additional sink, which interacts with the donor, describes the leakage of the electron from the RC. By manipulating the densities of the donor and acceptor states, or the tunneling rates, Γ_1 and Γ_2, (see below), one can fit the asymptotic behavior of the ET efficiency, η_2, for the acceptor ($0 \leq \eta_2 \leq 1$) with its experimental value. This approach is used for modeling the dynamics of the ET in photosynthetic complexes. (See, for example, [13,14], and references therein.)

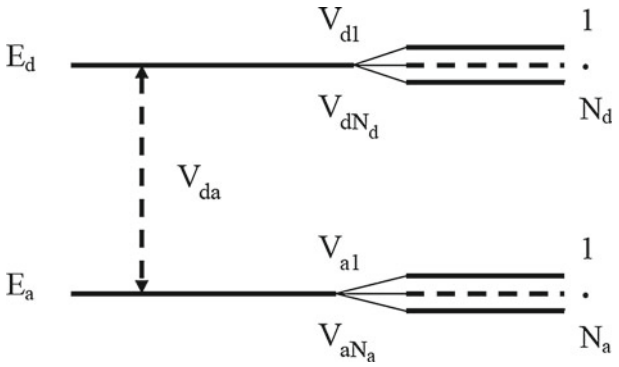

Fig. 13 Schematic of our modified model consisting of donor and acceptor discrete energy levels, with the donor and acceptor coupled to independent sink reservoirs with nearly continuous spectrum

The Hamiltonian of the system can be written as

$$\begin{aligned} H_t = {} & E_d|d\rangle\langle d| + E_a|a\rangle\langle a| + \frac{V}{2}(|d\rangle\langle a| + |a\rangle\langle d|) \\ & + \sum_{i=1}^{N_d}(E_i|i\rangle\langle i| + V_{di}|d\rangle\langle i| + V_{id}|i\rangle\langle d|) \\ & + \sum_{j=1}^{N_a}\left(E_j|j\rangle\langle j| + V_{aj}|a\rangle\langle j| + V_{ja}|j\rangle\langle a|\right), \end{aligned} \tag{47}$$

where $E_i(E_j)$ are energy levels of the sinks coupled with the donor (acceptor), and $V_{da} = V/2$.

After the transition to the continuum spectra of the sinks, the system is governed by the effective non-Hermitian Hamiltonian can, $\tilde{\mathscr{H}} = \mathscr{H} - i\mathscr{W}$, where

$$\mathscr{H} = \varepsilon_1|1\rangle\langle 1| + \varepsilon_2|2\rangle\langle 2| + \frac{V}{2}(|1\rangle\langle 2| + |2\rangle\langle 1|), \tag{48}$$

where $\mathscr{H}$ is the dressed donor-acceptor Hamiltonian and

$$\mathscr{W} = \frac{1}{2}(\Gamma_1|1\rangle\langle 1| + \Gamma_2|2\rangle\langle 2|). \tag{49}$$

Passing from Eq. (47) to Eqs. (48)–(49) we have changed $|d\rangle \to |1\rangle$ and $|a\rangle \to |2\rangle$. (See Appendix A.)

The dynamics of the system is described by the Liouville equation,

$$i\dot{\rho} = [\mathscr{H}, \rho] - i\{\mathscr{W}, \rho\}, \tag{50}$$

Further, we assume that initially the electron occupies the upper level (donor), $\rho_{11}(0) = 1$ and $\rho_{22}(0) = 0$. With these initial conditions, the solution of the Eq. (50) for the

diagonal component of the density matrix is given by

$$\rho_{11}(t) = e^{-\Gamma t}\left|\left(\cos\frac{\Omega t}{2} - i\cos\theta\sin\frac{\Omega t}{2}\right)\right|^2, \tag{51}$$

$$\rho_{22}(t) = e^{-\Gamma t}\left|\sin\theta\sin\frac{\Omega t}{2}\right|^2, \tag{52}$$

where $\Gamma = (\Gamma_1 + \Gamma_2)/2$, $\Omega = \sqrt{V^2 + (\varepsilon + i\Delta)^2}$ being the complex Rabi frequency, $\Delta = (\Gamma_2 - \Gamma_1)/2$, $\cos\theta = (\varepsilon + i\Delta)/\Omega$, and $\sin\theta = V/\Omega$.

Setting $\Omega = \Omega_1 + i\Omega_2$, we obtain for $\rho_{22}(t)$ the simple analytical expression:

$$\rho_{22}(t) = \frac{V^2 e^{-\Gamma t}}{2(\Omega_1^2 + \Omega_2^2)}\left(\cosh\Omega_2 t - \cos\Omega_1 t\right). \tag{53}$$

We define the ET efficiency of trapping the electron in the acceptor's sink as

$$\eta_2(t) = \Gamma_2\int_0^t \rho_{22}(\tau)d\tau. \tag{54}$$

Inserting $\rho_{22}(t)$ into (54) and performing the integration, we obtain

$$\eta_2(t) = \frac{\Gamma_2}{\Gamma_1 + \Gamma_2}\left(1 - \frac{e^{-\Gamma t}}{\Gamma(\Omega_1^2 + \Omega_2^2)}\left((\Gamma^2 + \Omega_1^2)(\Gamma\cosh\Omega_2 t + \Omega_2\sinh\Omega_2 t)\right.\right.$$
$$\left.\left. - (\Gamma^2 - \Omega_2^2)(\Gamma\cos\Omega_1 t - \Omega_1\sin\Omega_1 t)\right)\right). \tag{55}$$

From here it follows $\eta_2(t) \to \eta_0$, as $t \to \infty$, where

$$\eta_0 = \frac{\Gamma_2}{\Gamma_1 + \Gamma_2}. \tag{56}$$

4.1 Noise-assisted electron transfer

In the presence of classical diagonal noise, described by $\lambda_n = g_n\xi(t)$, the effective non-Hermitian Hamiltonian can be written as

$$\tilde{\mathscr{H}} = \sum_n\left(\varepsilon_n + g_n\xi(t) - i\frac{\Gamma_n}{2}\right)|n\rangle\langle n| + \frac{V}{2}\sum_{m\neq n}|m\rangle\langle n|. \tag{57}$$

We describe the evolution of the system by the following differential equations:

$$\frac{d}{dt}\langle\rho_{11}\rangle = -\Re_\Gamma\left(\langle\rho_{11}\rangle - \langle\rho_{22}\rangle\right) - \Gamma_1\langle\rho_{11}\rangle, \tag{58}$$

$$\frac{d}{dt}\langle\rho_{22}\rangle = \Re_\Gamma\left(\langle\rho_{11}\rangle - \langle\rho_{22}\rangle\right) - \Gamma_2\langle\rho_{22}\rangle, \tag{59}$$

where $\Re_\Gamma = \lim_{t\to\infty}\Re(t)$ is given by

$$\Re_\Gamma = \frac{V^2\sqrt{2\pi}}{8D\sigma}\left(\exp\left(\frac{(\Gamma+i\varepsilon)^2}{2D^2\sigma^2}\right)\operatorname{erfc}\left(\frac{\Gamma+i\varepsilon}{\sqrt{2}D\sigma}\right) + \exp\left(\frac{(\Gamma-i\varepsilon)^2}{2D^2\sigma^2}\right)\operatorname{erfc}\left(\frac{\Gamma-i\varepsilon}{\sqrt{2}D\sigma}\right)\right). \tag{60}$$

The motivation to use this simplified description is as follows. As was shown in Sec. III, approximation of integro-differential equations by the system of differential equations is valid for $v \le D\sigma$. In addition, since the ET rate reaches its asymptotic value, $\Re(t) \to \Re_\Gamma$, quite rapidly, at $t \approx 0.1$ ps, we can use the asymptotic rates, $\Re_\Gamma$, instead of $\Re(t)$. This allows us to use the analytical solutions to describe tunneling to the sinks with very high degree of accuracy.

The solution of Eqs. (58)–(59), with the initial conditions, $\langle\rho_{11}(0)\rangle = 1$ and $\langle\rho_{22}(0)\rangle = 0$, is

$$\langle\rho_{11}(t)\rangle = \left(\frac{1}{2} - \frac{\Delta}{2\sqrt{\Re_\Gamma^2+\Delta^2}}\right)e^{-\Re_1 t} + \left(\frac{1}{2} + \frac{\Delta}{2\sqrt{\Re_\Gamma^2+\Delta^2}}\right)e^{-\Re_2 t}, \tag{61}$$

$$\langle\rho_{22}(t)\rangle = \frac{\Re_\Gamma}{2\sqrt{\Re_\Gamma^2+\Delta^2}}\left(e^{-\Re_2 t} - e^{-\Re_1 t}\right), \tag{62}$$

where $\Re_{1,2} = \Re_\Gamma + \Gamma \pm \sqrt{\Re_\Gamma^2+\Delta^2}$ and $\Delta = (\Gamma_2-\Gamma_1)/2$.

The computation of the ET efficiency of tunneling in the acceptor's sink yields

$$\eta_2(t) = \frac{\Gamma_2\Re_\Gamma}{\Re_1\Re_2}\left(1 - e^{-\frac{(\Re_1+\Re_2)t}{2}}\left(\cosh\frac{(\Re_1-\Re_2)t}{2} + \frac{\Re_1+\Re_2}{\Re_1-\Re_2}\sinh\frac{(\Re_1-\Re_2)t}{2}\right)\right). \tag{63}$$

From here it follows, as $t \to \infty$,

$$\eta_2(t) \to \eta_r = \frac{\Gamma_2\Re_\Gamma}{\Re_1\Re_2}. \tag{64}$$

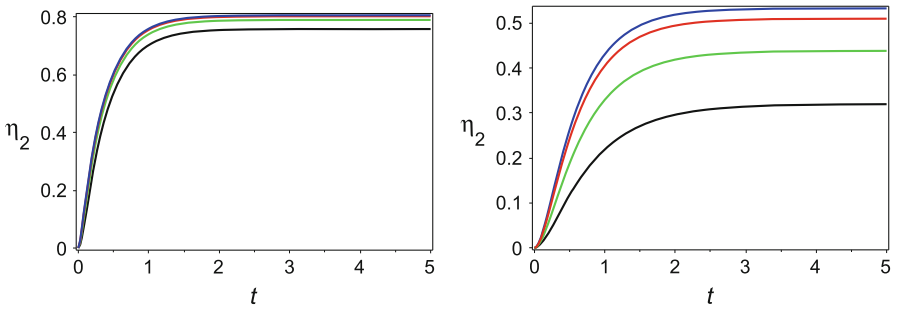

Fig. 14 (Color online) Time dependence (in ps) of the ET efficiency, $\eta_2(t)$ ($\Gamma_1 = 1\,\mathrm{ps}^{-1}$, $\Gamma_2 = 5\,\mathrm{ps}^{-1}$). *Blue line*: $\varepsilon = 0$, *red line*: $\varepsilon = 20\,\mathrm{ps}^{-1}$, *green line*: $\varepsilon = 40\,\mathrm{ps}^{-1}$, *black line*: $\varepsilon = 60\,\mathrm{ps}^{-1}$. *Left*: $V = 40\,\mathrm{ps}^{-1}$, $D\sigma = 40\,\mathrm{ps}^{-1}$. *Right*: $V = 10\,\mathrm{ps}^{-1}$, $D\sigma = 40\,\mathrm{ps}^{-1}$

Comparing the obtained results with the ET efficiency without noise, $\eta_0 = \Gamma_2/(\Gamma_1 + \Gamma_2)$, (see Eq. (56)), we obtain

$$\eta_r = \eta_0 \frac{2\Gamma\Re_\Gamma}{2\Gamma\Re_\Gamma + \Gamma^2 - \Delta^2}. \tag{65}$$

This can be represented in the form

$$\eta_r = \eta_0 \frac{(\Gamma_1 + \Gamma_2)\Re_\Gamma}{(\Gamma_1 + \Gamma_2)\Re_\Gamma + \Gamma_1\Gamma_2}. \tag{66}$$

From here it follows, that when $\Re_\Gamma \gg \Gamma_1\Gamma_2/(\Gamma_1 + \Gamma_2)$ the ET efficiency $\eta_r \approx \eta_0$. Generally, the ET efficiency with the presence of noise cannot exceed the ET efficiency without noise, $\eta_r \leq \eta_0$.

In Fig. 14, we present the results of numerical simulations of the ET efficiency when two sinks are taken into account. As one can see from Eq. (65), the asymptotic value for the ET efficiency, for chosen values of $\Gamma_{1,2}$, must satisfy the condition, $\eta_{rc} \leq \eta_0 \approx 83.3\,\%$. As one can see, the asymptotic value of η_{rc} is close enough to η_0, for chosen in Fig. 14 (left), parameters corresponding to black line. We also would like to mention that, as the results presented in Fig. 14 (left) demonstrate, the saturation of $\eta_2(t)$ happens fast enough, at $t \approx 2\,\mathrm{ps}$.

5 Conclusion and discussions

In this paper, we analyzed analytically and numerically the simplest model of the electron transfer (ET) between two protein sites, donor and acceptor, in the presence of classical (external) noise that is characterized by its amplitude and its correlation time. The noise is described by the well-known model of two-level fluctuators. We also included in our model two sinks which are represented by quasi-degenerate manifolds of electron energy levels. The sinks are directly coupled to the donor and acceptor states. This is done using the well-known Weisskopf–Wigner model [25–27].

When both noise and sinks influence the ET, the electron dynamics becomes rather complicated, and is generally described by a system of integro-differential equations. We derive the conditions for which a simplified system of ordinary differential equations can be used.

Our approach is rigorous in the sense that all approximations are controlled and justified. We obtain analytically and numerically the optimal ET rates and efficiency for both sharp and flat redox potential. In particular, we show that even for flat redox potential a sink associated with the acceptor can provide high enough efficiency of population the acceptor, which bosonic environment (or noise) can not do. Experimental verification of this result will represent a significant interest. We compare our approach for the ET rates with the results followed from the Marcus theory.

Our results can be used for analyzing and engineering optimal properties of photosynthetic bio-complexes.

Acknowledgments This work was carried out under the auspices of the National Nuclear Security Administration of the U.S. Department of Energy at Los Alamos National Laboratory under Contract No. DE-AC52-06NA25396. RTS acknowledges the U.S. Department of Energy-DE-SC0001295 for support of research regarding the organization of electron donors and acceptors in reaction center complexes. AIN acknowledges the support from the CONACyT, Grant No. 15349.

Appendix A: Non-Hermitian effective Hamiltonian

We consider the time-dependent Hamiltonian of a N-level system coupled with independent sinks through each level:

$$\begin{aligned}\mathscr{H}(t) = &\sum_{n=1}^{N} \epsilon_n(t)|n\rangle\langle n| + \sum_{m\neq n} \beta_{nm}(t)|n\rangle\langle m| \\ &+ \sum_{n=1}^{N}\sum_{i_n=1}^{N_n} \left(E_{i_n}|i_n\rangle\langle i_n| + V_{ni_n}|n\rangle\langle i_n| + V_{i_n n}|i_n\rangle\langle n|\right), \end{aligned} \tag{67}$$

where $m, n = 1, 2, \ldots, N$. We assume that the sinks are sufficiently dense, so that one can perform an integration instead of a summation. Then we have,

$$\begin{aligned}\mathscr{H}(t) = &\sum_{n} \epsilon_n(t)|n\rangle\langle n| + \sum_{m\neq n} \beta_{mn}(t)|n\rangle\langle m| \\ &+ \sum_{n}\left(\int \alpha_n(E)|n\rangle\langle E|g_n(E)dE + \text{h.c.}\right) + \sum_{n}\int E|E\rangle\langle E|g_n(E)dE \end{aligned} \tag{68}$$

where $g_n(E)$ is the density of states, and $V_{ni_n} \to \alpha_n(E)$.

With the state vector written as

$$|\psi\rangle = \sum_n \left(c_n(t)|n\rangle + \int c_{nE}(t)|E\rangle g_n(E) dE \right), \tag{69}$$

the Schrödinger equation,

$$i \frac{\partial |\psi(t)\rangle}{\partial t} = \mathscr{H}|\psi(t)\rangle, \tag{70}$$

takes the form

$$i\dot{c}_n(t) = E(t)c_n(t) + \sum_{m\neq n} \beta_{nm}(t)c_m(t) + \int_0^\infty \alpha_n^*(E)c_{nE}(t)g_n(E)dE \tag{71}$$

$$i\dot{c}_{nE}(t) = Ec_E(t) + \alpha_n(E)c_n(t). \tag{72}$$

In order to eliminate the continuum amplitudes from the equations for the discrete states, we first apply the Laplace transformation:

$$c_n(t) = \int_0^\infty e^{-st} c_n(s) ds, \tag{73}$$

$$c_{nE}(t) = \int_0^\infty e^{-st} c_{nE}(s) ds. \tag{74}$$

Then, from Eq. (72) we obtain

$$(s + iE)c_{nE}(s) = -i\alpha_n(E)c_n(s). \tag{75}$$

This yields $c_E(s) = -i\alpha_n(E)c_2(s)/(s + iE)$. Inserting this expression for $c_E(s)$ into Eq. (71), we obtain the following system of integro-differential equations, describing the non-Markovian dynamics of the TLS,

$$i\dot{c}_n(t) = Ec_n(t) + \sum_{n\neq m} \beta_{nm}(t)c_m(t) - i \int_0^\infty c_n(s)e^{-st} ds \int \frac{|\alpha_n(E)|^2 g_n(E)\, dE_n}{s + iE}. \tag{76}$$

To proceed further, we change the variable in the last integral, $s \to -E'$, so that

$$\int \frac{|\alpha_n(E)|^2 g_n(E)\, dE}{s + iE} \to -i \int \frac{|\alpha_n(E)|^2 g_n(E)\, dE_n}{E - E'} \tag{77}$$

The next step is to use the identity

$$\frac{1}{x-x'+i0} = \mathscr{P}\left\{\frac{1}{x-x'}\right\} - i\pi\delta(x-x'), \tag{78}$$

where $\mathscr{P}$ = Principal value. This yields

$$\int \frac{|\alpha_n(E)|^2 g_n(E)\,dE}{E-E'} = \Delta(E') - \frac{i}{2}\Gamma_n(E'), \tag{79}$$

where

$$\Delta(E') = \mathscr{P}\int \frac{|\alpha_n(E)|^2 g_n(E)\,dE}{E-E'}, \tag{80}$$

$$\Gamma_n(E') = 2\pi\int |\alpha_n(E)|^2 g_n(E)\delta(E-E')\,dE. \tag{81}$$

Now using the Weisskopf–Wigner pole approximation, we evaluate the integrals as follows [25,26,47]:

$$\Delta(E') \approx \Delta(\epsilon_n) = \mathscr{P}\int \frac{|\alpha_n(E)|^2 g_n(E)dE}{E-\epsilon_n}, \tag{82}$$

$$\Gamma_n(E') \approx \Gamma_n(\epsilon_n) = 2\pi\int |\alpha_n(E)|^2 g_n(E)\delta(E-\epsilon_n)\,dE = 2\pi g_n(\epsilon_n)|\alpha_n(\epsilon_n)|^2. \tag{83}$$

The Weisskopf–Wigner pole approximation basically corresponds to the assumption that the coupling constant to the continuum is a smoothly varying function of the energy, e.g. the continuum is treated as a single discrete level.

Inserting (82) into Eq. (71), we obtain

$$i\dot{c}_n(t) = \varepsilon_n(t)c_n(t) + \sum_{m\neq n}\beta_{nm}(t)c_m(t) - \frac{i\Gamma_n}{2}c_n(t), \tag{84}$$

where $\Gamma_n = \Gamma_n(E_n)$ and $\varepsilon(t) = \epsilon_n(t) - \Delta(E_n)$.

Writing $|\psi_N\rangle = \sum_n c_n(t)|n\rangle$, we find that the dynamics of the N-level system interacting with the continuum is described by the Schrödinger equation,

$$i\frac{\partial|\psi_N(t)\rangle}{\partial t} = \tilde{\mathscr{H}}|\psi_N(t)\rangle, \tag{85}$$

where $\tilde{\mathscr{H}} = \mathscr{H} - i\mathscr{W}$ is the effective non-Hermitian Hamiltonian,

$$\mathscr{H} = \sum_n \varepsilon_n|n\rangle\langle n| + \sum_{m\neq n}\beta_{mn}(t)|m\rangle\langle n| \tag{86}$$

being the dressed Hamiltonian, and

$$W = \frac{1}{2}\sum_n \Gamma_n |n\rangle\langle n|. \tag{87}$$

Equivalently, the dynamics of this system can be described by the Liouville equation,

$$i\dot{\rho} = \tilde{\mathscr{H}}\rho - \rho\tilde{\mathscr{H}}^\dagger = [\mathscr{H}, \rho] - i\{\mathscr{W}, \rho\}, \tag{88}$$

where ρ is the density matrix projected on the intrinsic states, and $\{\mathscr{W}, \rho\} = \mathscr{W}\rho + \rho\mathscr{W}$.

In particular case of the two-level system considered in this paper, the effective non-Hermitian Hamiltonian takes the form

$$\tilde{\mathscr{H}} = \frac{1}{2}\begin{pmatrix} 2\varepsilon_1 - i\Gamma_1 & V \\ V & 2\varepsilon_2 - i\Gamma_2 \end{pmatrix}. \tag{89}$$

Comments. The results of this section can be obtained using the standard Feshbach projection method [26,32–35].

Appendix B: Equation of motion for the average density matrix

In this Appendix, we derive from the Liouville equation, $i\dot{\rho} = [\tilde{\mathscr{H}}, \rho] - i\{\mathscr{W}, \rho\}$, the equation of motion for the average density matrix. We will use the interaction representation. Considering the off-diagonal elements as perturbations, so that $\tilde{\mathscr{H}} = \mathscr{H}_0 + V(t) - i\mathscr{W}$, where

$$\mathscr{H}_0 = \sum_n \varepsilon_n |n\rangle\langle n| + \sum_n \lambda_{nn}(t)|n\rangle\langle n|, \tag{90}$$

$$V(t) = \sum_{m\neq n} (V_{mn} + \lambda_{mn}(t))|m\rangle\langle n|, \tag{91}$$

$$\mathscr{W} = \frac{\Gamma_1}{2}|1\rangle\langle 1| + \frac{\Gamma_2}{2}|2\rangle\langle 2|, \tag{92}$$

we obtain the following equations of motion:

$$\dot{\tilde{\rho}}_{11} = i(\tilde{\rho}_{12}\tilde{V}_{21} - \tilde{V}_{12}\tilde{\rho}_{21}) - \Gamma_1\tilde{\rho}_{11}, \tag{93}$$

$$\dot{\tilde{\rho}}_{22} = i(\tilde{\rho}_{21}\tilde{V}_{12} - \tilde{V}_{21}\tilde{\rho}_{12}) - \Gamma_2\tilde{\rho}_{22}, \tag{94}$$

$$\dot{\tilde{\rho}}_{12} = i\tilde{V}_{12}(\tilde{\rho}_{11} - \tilde{\rho}_{22}) - \Gamma\tilde{\rho}_{12}, \tag{95}$$

$$\dot{\tilde{\rho}}_{21} = i\tilde{V}_{21}(\tilde{\rho}_{11} - \tilde{\rho}_{22}) - \Gamma\tilde{\rho}_{21}, \tag{96}$$

where $\Gamma = (\Gamma_1 + \Gamma_2)/2$,

$$\tilde{\rho} = T\left(e^{i\int_0^t H_0(\tau)d\tau}\right)\rho T\left(e^{-i\int_0^t H_0(\tau)d\tau}\right), \tag{97}$$

and

$$\tilde{V} = T\left(e^{i\int_0^t H_0(\tau)d\tau}\right)VT\left(e^{-i\int_0^t H_0(\tau)d\tau}\right). \tag{98}$$

Using Eqs. (93)–(96), we obtain

$$\tilde{\rho}_{11}(t) = \tilde{\rho}_{11}(0) + i\int_0^t e^{-\Gamma_1(t-t')}(\tilde{\rho}_{12}(t')\tilde{V}_{21}(t') - \tilde{V}_{12}(t')\tilde{\rho}_{21}(t'))dt', \tag{99}$$

$$\tilde{\rho}_{22}(t) = \tilde{\rho}_{22}(0) + i\int_0^t e^{-\Gamma_2(t-t')}(\tilde{\rho}_{21}(t')\tilde{V}_{12}(t') - \tilde{V}_{21}(t')\tilde{\rho}_{12}(t'))dt', \tag{100}$$

$$\tilde{\rho}_{12}(t) = \tilde{\rho}_{12}(0) + i\int_0^t e^{-\Gamma(t-t')}\tilde{V}_{12}(t')(\tilde{\rho}_{11}(t') - \tilde{\rho}_{22}(t'))dt', \tag{101}$$

$$\tilde{\rho}_{21}(t) = \tilde{\rho}_{21}(0) + i\int_0^t e^{-\Gamma(t-t')}\tilde{V}_{21}(t')(\tilde{\rho}_{11}(t') - \tilde{\rho}_{22}(t'))dt'. \tag{102}$$

We assume that initially $\tilde{\rho}_{12}(0) = \tilde{\rho}_{21}(0) = 0$. Now, inserting (99)–(102) into Eqs. (93)–(96), and taking into account that $\tilde{\rho}_{11} = \rho_{11}$ and $\tilde{\rho}_{22} = \rho_{22}$, we obtain the following system of integro-differential equations,

$$\begin{aligned}\dot{\rho}_{11}(t) = &-\int_0^t e^{-\Gamma(t-t')}\left(\tilde{V}_{21}(t)\tilde{V}_{12}(t') + \tilde{V}_{21}(t')\tilde{V}_{12}(t)\right)\left(\rho_{11}(t') - \rho_{22}(t')\right)dt' \\ &-\Gamma_1\rho_{11}(t),\end{aligned} \tag{103}$$

$$\begin{aligned}\dot{\rho}_{22}(t) = &\int_0^t e^{-\Gamma(t-t')}\left(\tilde{V}_{21}(t)\tilde{V}_{12}(t') + \tilde{V}_{21}(t')\tilde{V}_{12}(t)\right)\left(\rho_{11}(t') - \rho_{22}(t')\right)dt' \\ &-\Gamma_2\rho_{22}(t),\end{aligned} \tag{104}$$

$$\begin{aligned}\dot{\tilde{\rho}}_{12}(t) = &-\int_0^t \left(e^{-\Gamma_1(t-t')} + e^{-\Gamma_2(t-t')}\right)\left(\tilde{V}_{21}(t')\tilde{\rho}_{12}(t') - \tilde{V}_{12}(t')\tilde{\rho}_{21}(t')\right)\tilde{V}_{12}(t)dt' \\ &-\Gamma\rho_{12}(t) + i\tilde{V}_{12}(t)(\rho_{11}(0) - \rho_{22}(0)),\end{aligned} \tag{105}$$

$$\dot{\tilde{\rho}}_{21}(t) = -\int_0^t \left(e^{-\Gamma_1(t-t')} + e^{-\Gamma_2(t-t')}\right)\left(\tilde{V}_{21}(t')\tilde{\rho}_{12}(t') - \tilde{V}_{12}(t')\tilde{\rho}_{21}(t')\right)\tilde{V}_{21}(t)dt'$$
$$-\Gamma\rho_{21}(t) + i\tilde{V}_{21}(t)(\rho_{11}(0) - \rho_{22}(0)). \tag{106}$$

For the average components of the density matrix this yields

$$\frac{d}{dt}\langle\rho_{11}(t)\rangle = -\int_0^t e^{-\Gamma(t-t')}\Big\langle\left(\tilde{V}_{21}(t)\tilde{V}_{12}(t') + \tilde{V}_{21}(t')\tilde{V}_{12}(t)\right)$$
$$\times\left(\rho_{11}(t') - \rho_{22}(t')\right)\Big\rangle dt' - \Gamma_1\langle\rho_{11}(t)\rangle, \tag{107}$$
$$\frac{d}{dt}\langle\rho_{22}(t)\rangle = \int_0^t e^{-\Gamma(t-t')}\Big\langle\left(\tilde{V}_{21}(t)\tilde{V}_{12}(t') + \tilde{V}_{21}(t')\tilde{V}_{12}(t)\right)\left(\rho_{11}(t') - \rho_{22}(t')\right)\Big\rangle dt'$$
$$-\Gamma_2\langle\rho_{22}(t)\rangle, \tag{108}$$
$$\frac{d}{dt}\langle\rho_{12}(t)\rangle = -\int_0^t \left(e^{-\Gamma_1(t-t')} + e^{-\Gamma_2(t-t')}\right)$$
$$\times\Big\langle\left(\tilde{V}_{21}(t')\tilde{\rho}_{12}(t') - \tilde{V}_{12}(t')\tilde{\rho}_{21}(t')\right)\tilde{V}_{12}(t)\Big\rangle dt' - \Gamma\langle\rho_{12}(t)\rangle$$
$$+i\langle\tilde{V}_{12}(t)\rangle(\rho_{11}(0) - \rho_{22}(0)), \tag{109}$$
$$\frac{d}{dt}\langle\rho_{21}(t)\rangle = -\int_0^t + \left(e^{-\Gamma_1(t-t')} + e^{-\Gamma_2(t-t')}\right)$$
$$\times\Big\langle\left(\tilde{V}_{21}(t')\tilde{\rho}_{12}(t') - \tilde{V}_{12}(t')\tilde{\rho}_{21}(t')\right)\tilde{V}_{21}(t)\Big\rangle dt' - \Gamma\langle\rho_{21}(t)\rangle$$
$$+i\langle\tilde{V}_{21}(t)\rangle(\rho_{11}(0) - \rho_{22}(0)), \tag{110}$$

where the average $\langle\ \rangle$ is taken over the random process describing noise.

In the spin-fluctuator model of noise with the number of fluctuators, $\mathcal{N} \gg 1$, one has the following relations for the splitting of correlations [43],

$$\Big\langle\left(\tilde{V}_{21}(t)\tilde{V}_{12}(t') + \tilde{V}_{21}(t')\tilde{V}_{12}(t)\right)\left(\tilde{\rho}_{11}(t') - \tilde{\rho}_{22}(t')\right)\Big\rangle$$
$$= \left(\Big\langle\tilde{V}_{21}(t)\tilde{V}_{12}(t')\Big\rangle + \Big\langle\tilde{V}_{21}(t')\tilde{V}_{12}(t)\Big\rangle\right)\left(\langle\tilde{\rho}_{11}(t')\rangle - \langle\tilde{\rho}_{22}(t')\rangle\right), \tag{111}$$

and so on. Employing (111), we obtain the following system of integro-differential equations for the average components of the density matrix,

$$\frac{d}{dt}\langle\rho_{11}(t)\rangle = -\int_0^t e^{-\Gamma(t-t')}\big(\langle\tilde{V}_{21}(t)\tilde{V}_{12}(t')\rangle + \langle\tilde{V}_{21}(t')\tilde{V}_{12}(t)\rangle\big)\big(\langle\rho_{11}(t')\rangle - \langle\rho_{22}(t')\rangle\big)dt' - \Gamma_1\langle\rho_{11}(t)\rangle, \tag{112}$$

$$\frac{d}{dt}\langle\rho_{22}(t)\rangle = \int_0^t e^{-\Gamma(t-t')}\big(\langle\tilde{V}_{21}(t)\tilde{V}_{12}(t')\rangle + \langle\tilde{V}_{21}(t')\tilde{V}_{12}(t)\rangle\big)\big(\langle\rho_{11}(t')\rangle - \langle\rho_{22}(t')\rangle\big)dt' - \Gamma_2\langle\rho_{22}(t)\rangle, \tag{113}$$

$$\begin{aligned}\frac{d}{dt}\langle\tilde{\rho}_{12}(t)\rangle &= i\langle\tilde{V}_{12}(t)\rangle(\rho_{11}(0)-\rho_{22}(0)) \\ &\quad -\int_0^t \left(e^{-\Gamma_1(t-t')}+e^{-\Gamma_2(t-t')}\right)\langle\tilde{V}_{12}(t)\tilde{V}_{21}(t')\rangle\langle\tilde{\rho}_{12}(t')\rangle dt' \\ &\quad +\int_0^t \left(e^{-\Gamma_1(t-t')}+e^{-\Gamma_2(t-t')}\right)\langle\tilde{V}_{12}(t)\tilde{V}_{12}(t')\rangle\langle\tilde{\rho}_{21}(t')\rangle dt' - \Gamma\langle\tilde{\rho}_{12}(t)\rangle,\end{aligned} \tag{114}$$

$$\begin{aligned}\frac{d}{dt}\langle\tilde{\rho}_{21}(t)\rangle &= i\langle\tilde{V}_{21}(t)\rangle(\rho_{11}(0)-\rho_{22}(0)) \\ &\quad -\int_0^t \left(e^{-\Gamma_1(t-t')}+e^{-\Gamma_2(t-t')}\right)\langle\tilde{V}_{21}(t)\tilde{V}_{21}(t')\rangle\langle\tilde{\rho}_{12}(t')\rangle dt' \\ &\quad +\int_0^t \left(e^{-\Gamma_1(t-t')}+e^{-\Gamma_2(t-t')}\right)\langle\tilde{V}_{21}(t)\tilde{V}_{12}(t')\rangle\langle\tilde{\rho}_{21}(t')\rangle dt' - \Gamma\langle\tilde{\rho}_{21}(t)\rangle.\end{aligned} \tag{115}$$

Using these relations, we obtain the following system of integro-differential equations for the diagonal components of the density matrix,

$$\frac{d}{dt}\langle\rho_{11}(t)\rangle = -\int_0^t K(t,t')\left(\langle\rho_{11}(t')\rangle - \langle\rho_{22}(t')\rangle\right)dt' - \Gamma_1\langle\rho_{11}(t)\rangle, \tag{116}$$

$$\frac{d}{dt}\langle\rho_{22}(t)\rangle = \int_0^t K(t,t')\left(\langle\rho_{11}(t')\rangle - \langle\rho_{22}(t')\rangle\right)dt' - \Gamma_2\langle\rho_{22}(t)\rangle, \tag{117}$$

where the kernel is given by

$$K(t,t') = e^{-\Gamma(t-t')}\left(\left\langle\tilde{V}_{21}(t)\tilde{V}_{12}(t')\right\rangle + \left\langle\tilde{V}_{21}(t')\tilde{V}_{12}(t)\right\rangle\right). \tag{118}$$

For the diagonal noise, so that $\lambda_{mn} = 0\,(m \neq n)$, the kernel can be recast as

$$K(t-t') = |V_{12}|^2 e^{-\Gamma(t-t')}\left(e^{i\varepsilon_{12}(t-t')}\left\langle e^{-i\kappa(t-t')}\right\rangle + e^{-i\varepsilon_{12}(t-t')}\left\langle e^{i\kappa(t-t')}\right\rangle\right), \quad (119)$$

where $\varepsilon_{12} = \varepsilon_1 - \varepsilon_2$, $\kappa(t-t') = D\int_0^{t-t'}\xi(\tau)d\tau$ and $D = |g_1 - g_2|$.

Applying the cumulant expansion, the generating functional can be recast in terms of the line shape function and correlation function

$$\left\langle e^{i\kappa(t-t')}\right\rangle = e^{i\lambda_0(t-t') - \langle\kappa^2(t-t')\rangle/2}, \quad (120)$$

where $\lambda_0 = D\langle\xi(0)\rangle$ and

$$\langle\kappa^2(t-t')\rangle = 2D^2\int_0^{t-t'}d\tau'\int_0^{\tau'}d\tau''\chi(\tau'-\tau''). \quad (121)$$

Employing Eqs. (120)–(121), we obtain

$$K(t-t') = \frac{V^2}{2}\cos(\varepsilon(t-t'))\exp\left(-\Gamma(t-t') - D^2\int_0^{t-t'}d\tau'\int_0^{\tau'}d\tau''\chi(\tau'-\tau'')\right), \quad (122)$$

where $\varepsilon = \varepsilon_{12} - \lambda_0$.

Using the results obtained in Sec. III, one can show that for $V < D\sigma$ the system of integro-differential Eqs. (116)–(117) can be approximated by the following system of ordinary differential equations:

$$\frac{d}{dt}\langle\rho_{11}\rangle = -\Re(t)\left(\langle\rho_{11}\rangle - \langle\rho_{22}\rangle\right) - \Gamma_1\langle\rho_{11}\rangle, \quad (123)$$

$$\frac{d}{dt}\langle\rho_{22}\rangle = \Re(t)\left(\langle\rho_{11}\rangle - \langle\rho_{22}\rangle\right) - \Gamma_2\langle\rho_{22}\rangle, \quad (124)$$

where $\Re(t) = \int_0^t \tau K(\tau)d\tau$. Performing the integration we obtain

$$\Re(t) = \frac{\sqrt{\pi}q}{4p}\exp\left(\frac{q^2}{4p^2}\right)\left(\operatorname{erf}\left(\frac{q}{2p} + pt\right) - \operatorname{erf}\left(\frac{q}{2p}\right)\right) + \frac{\sqrt{\pi}\bar{q}}{4p}\exp\left(\frac{\bar{q}^2}{4p^2}\right)\left(\operatorname{erf}\left(\frac{\bar{q}}{2p} + pt\right) - \operatorname{erf}\left(\frac{\bar{q}}{2p}\right)\right), \quad (125)$$

where $p = D\sigma/\sqrt{2}$, $q = \Gamma + i\varepsilon$, $\bar{q} = \Gamma - i\varepsilon$, and $\operatorname{erf}(z)$ is the error function [44].

References

1. R. Blankenship, *Molecular Mechansms of Photosynthesus* (World Scientific, London, 2002)
2. T. Gustafson, R. Sayre, PNAS **99**, 4091 (2002)
3. L. Xiong, M. Seibert, A. Gusev, M. Wasielewski, C. Hemann, C. Hille, R. Sayre, J. Phys. Chem. B **108**, 16904 (2004)
4. Z. Perrine, R. Sayre, Biochemistry **50**, 1454 (2011)
5. K.L.M. Lewis, F.D. Fuller, J.A. Myers, C.F. Yocum, S. Mukamel, D. Abramavicius, J.P. Ogilvie, J. Phys. Chem. A **117**, 34 (2012)
6. G. Engel, T. Calhoun, E. Read, T. Ahn, T. Mancal, Y. Cheng, R. Blankenship, G. Fleming, Nat. Lett. **446**, 782 (2007)
7. A. Ishizaki, G.R. Fleming, J. Chem. Phys. **130**, 234110 (2009)
8. E. Collini, C. Wong, K. Wilk, P. Curmi, P. Brumer, G. Scholes, Nat. Lett. **463**, 644 (2010)
9. G. Panitchayangkoon, D. Hayes, K. Fransted, J. Caram, E. Harel, J. Wenb, R. Blankenship, G. Engel, PNAS USA **107**, 12766 (2010)
10. A. Ishizaki, G. Fleming, PNAS **106**, 17255 (2009)
11. P. Rebentrost, M. Mohseni, I. Kassal, S. Lloyd, A. Aspuru-Guzik, New J. Phys. **11**(3), 033003 (2009)
12. G. Celardo, F. Borgonovi, M. Merkli, V. Tsifrinovich, G. Berman, J. Phys. Chem. **116**, 22105 (2012)
13. R. Pinčák, M. Pudlak, Phys. Rev. E **64**, 031906 (2001)
14. M. Pudlak, R. Pincak, J. Biol. Phys. **36**, 273 (2010)
15. R. Marcus, N. Sutin, Biochimica et Biophys. Acta **811**, 265 (1985)
16. X. Hu, A. Damjanovic, T. Ritz, K. Schulten, Proc. Natl. Acad. Sci. USA **95**, 5935 (1998)
17. M. Merkli, G.P. Berman, R. Sayre, J. Math. Chem. **51**, 890 (2013)
18. E. Collini, C. Wong, K. Wilk, P. Curmi, P. Brumer, G. Scholes, Nat. Lett. **463**, 644 (2010)
19. K. Schulten, M. Tesch, Chem. Phys. **158**, 421 (1991)
20. D. Xu, K. Schulten, Chem. Phys. **182**, 91 (1994)
21. S. Skourtis, D. Waldeck, D. Beratan, Annu. Rev. Phys. Chem. **64**, 461 (2010)
22. B. McMahon, P. Fenimore, M. LaBute, in *Fluctuations and Noise in Biological, Biophysical, and Biomedical Systems, Proceedings of SPIE, vol. 5110*, ed. by S.M. Bezrukov, H. Frauenfelder, F. Moss (2003), pp. 10–21
23. A. Bar-Even, J. Paulsson, N. Maheshri, M. Carmi, E. O'Shea, Y. Pilpel, N. Barkai, Nat. Genet. **38**, 636 (2006)
24. A. Thilagam, J. Chem. Phys. **136**, 065104 (2012)
25. V.F. Weisskopf, E.P. Wigner, Z. Phys. **63**, 54 (1930)
26. S. Mukamel, *Principles of Nonlinear Optical Spectroscopy* (Oxford University Press, New York, 1995)
27. M.O. Scully, M.S. Zubairy, *Quantum Optics* (Cambridge University Press, Cambridge, 1997)
28. T.G. Dewey, J.G. Bann, Biophys. J. **63**, 594 (1992)
29. R. Grima, J. Chem. Phys. **132**, 185102 (2010)
30. P. Carlini, A.R. Bizzarri, S. Cannistraro, Phys. D **165**, 242 (2002)
31. M.S. Samoilov, G. Price, A.P. Arkin, Science's STKE, 2006, re17 (2006)
32. I. Rotter, Phys. Rev. E **64**, 036213 (2001)
33. I. Rotter, Rep. Prog. Phys. **54**(4), 635 (1991)
34. I. Rotter, J. Phys. A **42**, 153001 (2009)
35. A. Volya, V. Zelevinsky, Phys. Rev. Lett. **94**, 052501 (2005)
36. A.I. Nesterov, G.P. Berman, A.R. Bishop, Fortschr. Phys. **61**, 95 (2013)
37. M.V. Berry, Proc. R. Soc. A **392**, 45 (1984)
38. M.V. Berry, Czech. J. Phys. **54**, 1039 (2004)
39. V.D. Lakhno, Phys. Chem. Chem. Phys **4**, 2246 (2002)
40. A.W. Chin, A. Datta, F. Caruso, S.F. Huelga, M.B. Plenio, New J. Phys. **12**, 065002 (2010)
41. Y.M. Galperin, B.L. Altshuler, J. Bergli, D. Shantsev, V. Vinokur, Phys. Rev. B **76**, 064531 (2007)
42. J. Bergli, Y.M. Galperin, B.L. Altshuler, New J. Phys. **11**, 025002 (2009)
43. A.I. Nesterov, G.P. Berman, Phys. Rev. A **85**, 052125 (2012)
44. M. Abramowitz, I.A. Stegun (eds.), *Handbook of Mathematical Functions* (Dover, New York, 1965)
45. M. Takano, T. Takahashi, K. Nagayama, Phys. Rev. Lett. **80**, 5691 (1998)
46. M. Joyeux, S. Buyukdagli, M. Sanrey, Phys. Rev. E **75**, 061914 (2007)
47. E. Kyrola, J. Phys. B **19**, 1437 (1986)